ELSEVIER

Computational Materials Science 28 (2003) 574–586

COMPUTATIONAL MATERIALS SCIENCE

www.elsevier.com/locate/commatsci

Deformation and damage in Al/Al_2O_3

E. Soppa [a,*], S. Schmauder [a], G. Fischer [b], J. Brollo [a], U. Weber [a]

[a] *Staatliche Materialprüfungsanstalt (MPA) Universität Stuttgart, Pfaffenwaldring 32, 70569 Stuttgart, Germany*

[b] *Dortmunder Initiative zur rechnerintegrierten Fertigung (RIF) e.V., Joseph-von-Fraunhofer-Straße 20, 44227 Dortmund, Germany*

Abstract

Al/Al_2O_3-composites as an example of light weight materials are very interesting for many industrial applications because of a favourable combination of low density and improved mechanical properties. The prediction of the macroscopic mechanical behaviour of these materials related to their microstructure requires the knowledge of damage initiation and crack development under external loading conditions and, if present, residual stresses have to be taken into consideration. Different types of material degradation like particle/matrix-debonding, particle failure and matrix cracking can be observed in these types of metal matrix composites. The aim of the present work is to introduce damage criteria into a FE-microstructural model in order to foresee the degradation process in an Al_2O_3-particle reinforced Al(6061) composite during mechanical loading. Presently, the conventional fabrication route of the Al/Al_2O_3-composite is a metallurgical method with extrusion for homogenisation of the microstructure and final heat treatment to achieve a defined precipitation state. The influence of thermal residual stresses due to cooling down from annealing temperature on the deformation and damage initiation of Al(6061)/10vol%Al_2O_3-composites is investigated through finite element analyses using the experimentally mapped real microstructure as binary data. Especially, the stresses in the ceramic particles which are responsible for particle cracking and the hydrostatic stresses in the Al-matrix making the particle–matrix interface prone to debonding were analysed. The results show the importance of the thermal residual stresses with respect to damage criteria as obtained by micromechanical FE-calculations.

Keywords: Microstructure; Computer simulation; FE-method; Metal matrix composites (MMCs); Microgrid technique; Damage initiation; Residual stresses

1. Introduction

The understanding of the correlation between microstructure, deformation, damage initiation and damage development in composite materials is of major importance for engineering materials and their commercial use in automotive and aerospace systems. The degree of property improvement depends on morphological factors such as volume fraction, size, shape and spatial distribution of the reinforcements, in addition to the constituent material and interfacial properties.

Properties and performance of composite materials are related to their microstructures, which is in turn governed by the manufacturing process parameters. Reliable prediction of the mechanical

* Corresponding author. Tel.: +49-711-685-3056; fax: +49-711-685-2635.

E-mail address: ewa.soppa@mpa.uni-stuttgart.de (E. Soppa).

0927-0256/$ - see front matter © 2003 Elsevier B.V. All rights reserved.
doi:10.1016/j.commatsci.2003.08.034

response of the material using simulation tools requires to take into account such factors like: real microstructure, dimensions of the cut-outs chosen for the FE-models, realistic boundary conditions, residual stresses resulting from the production process and existing cracks and voids in the undeformed state as a consequence of the extrusion process.

A self-consistent model for studying deformation behaviour of MMCs with a random distribution of particles is presented in [18]. Micro- and mesomechanical approaches to the problem of damage in particles and matrix can be found in [18–29]. Different types of damage in MMCs: particle cracking and debonding are studied in Refs. [36,39,40]. The effects of particle cracking or debonding in metal matrix composites during loading have been investigated by several authors, e.g. [1–5]. They have established that the deformation behaviour of composites strongly depends on the damage progress and that particles with an overcritical size break first [6]. Most of the current models show a very sharp drop of stresses accompanying particle cracking because of an oversimplified microstructure, which is not realistic [2,3]. Modeling of the crack development in the matrix phase and particles as well as debonding at the same time has been simulated in steel and described in [7]. Some 2D and 3D simulations depending on the microstructure types have been performed for two-phase materials using the finite element method [8–10]. Geni [11] investigated damage initiation at the edges of SiC-particles in Al as well as crack propagation in the matrix using Gurson's model. Buffière et al. [61] found out that the cracking of SiC-particles during straining is underestimated by surface observation because of the partial relaxation of the residual stresses there. One of the first numerical work on the simulation of cracks in hard particles in WC/Co is given in Ref. [12]. The interaction between broken particles and particles with a crack along the interface as well as the interaction between holes [13] is still a subject of investigations. Description of the particle–crack interaction in the presence of residual stresses can be found in [5,14–17]. The magnitude and nature of residual stresses significantly affect the mechanical properties of MMCs [56] and may cause a higher flow stress in compression than in tension [60]. Information about the neutron diffraction measurements of the residual stresses in Al_2O_3 particles in undeformed samples and after compression can be found in [57]. Li et al. [58] analysed the residual stress distributions near the interfaces in a SiC/6061Al composite depending on different low temperature treatments and showed the effective method of reducing such stresses. The interaction between the crack tip and the particle depends strongly on the matrix properties. A crack which approaches a soft particle with a higher value of thermal expansion coefficient than the matrix phase will be attracted by the particle, whereas hard particles with a lower value of thermal expansion coefficient will deflect the crack [5,14–16]. In most MMCs the hard ceramic particles possess the lower value of the thermal expansion coefficient than the matrix phase resulting in crack deflection by particles [17,32,33]. The influence of the microstructure on the deformation and/or crack development has been simulated with help of the FE-method in case of Al/SiC [26,28], WC/Co [24], and Al/Si [21]. The crack shows a typical behaviour for the situation with existing high stress triaxiality state: building of voids at the crack tip, void growth and coalescence of voids at the crack tip leading finally to total failure of the component.

Measurements of local strains and the analysis of the strain distribution in two-phase Ag/Ni-composites depending on the macroscopical strain and the comparison with simulation results can be found in [30,31,34]. Bridging of the different length scales in experiment and simulation in order to show the influence of the microstructural features on the macro- or mesoscale on the local strain and/or stress distribution were described in [35]. A quantitative description of real microstructures and generating equivalent artificial microstructures has been performed in [37] for the example of fibres in a ceramic matrix. Ceramic particle rotation during the loading (tensile or compression) has been analysed in dependence of the particle's orientation [38]. Predictions of the damage initiation in different types of composites with metal, organic or ceramic matrices are presented in [41–46]. Le Pen and Baptiste [41] introduced damage in

Table 1
Chemical composition of Al(6061) [47]

Element	Cr	Cu	Fe	Mg	Mn	Si	Ti	Zn
Wt.%	0.04–0.35	0.15–0.4	0.7	0.8–1.2	0.15	0.4–0.8	0.15	0.25

an elasto-plastic micromechanical model for fatigue damage prediction by using a fibre failure criterion identified in in-situ tensile tests in the scanning electron microscope. An interfacial failure criterion as a linear combination of the normal and the shear stress has been introduced by Fitoussi [43] in order to predict the macroscopic mechanical behaviour of sheet-moulding-compound.

2. Material and microstructure

On the microlevel the studied composite material [1] Al(6061)/10vol%Al_2O_3 consists of two phases: metal matrix Al(6061) (Table 1) and 10 vol% of Al_2O_3 ceramic particles distributed in the matrix (Fig. 1). This material has been fabricated via metallurgical route, extruded and heat treated in a defined way to achieve a particular precipitation state (Table 2). Physical and mechanical data used in the FE-calculations are gathered in Table 3. Al_2O_3 particles deform only in an elastic region, whereas the Al-matrix shows an elasto-plastic deformation behaviour with a relatively low value of the yield stress of about $\sigma_0 = 105$ MPa. The experimental data concerning the stress–strain curve for Al(6061) used in the FE-calculations are known from experiment [59].

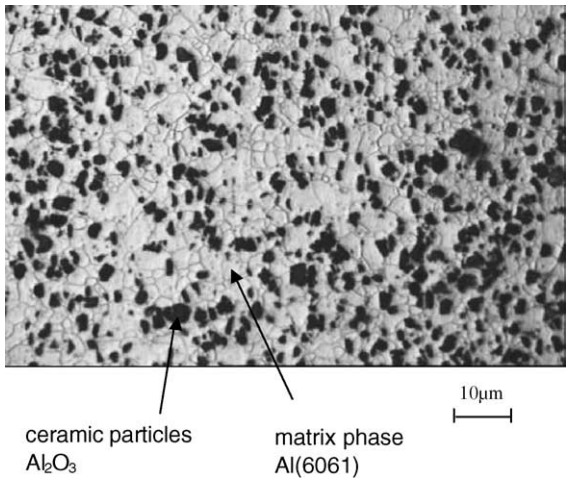

Fig. 1. Microstructure of Al(6061)/(10vol%)Al_2O_3, SEM.

Table 2
Thermal treatment T6 for defined precipitation state [47,59]

Treatment	Temperature	Time
Annealing	530 °C	30 min
Quenching till	Ambient temperature	
Annealing	160 °C	24 h
Natural aging	Ambient temperature	

3. Methods of investigations

A close combination of experiment and simulation has been achieved in this work. Experimental data like binary figures of the real microstructure, the stress–strain curve for the matrix bulk material as well as local displacements measured in a tensile test after certain deformation steps have been used as input data for the FE-calculations.

3.1. Tensile test and an object grating technique

A mechanically polished surface of the tensile specimen has been structured using a very fine grid of gold dots. The distance between the dots depends on the microstructure fineness. Regularly distributed dots guarantee a good contrast and

[1] Precipitates which exist in the matrix-phase and contribute to the work hardening are not considered here but are taken into account in the stress–strain curve for Al(6061) bulk material.

Table 3
Physical and mechanical data of Al(6061)/10vol%Al_2O_3

Phase	E (GPa)	ν	σ_0 (MPa)	σ_{max} (MPa)	ε_0	α[a] (1/K)
Al(6061)-matrix	68.3	0.33	105.0	170.0	0.048	2.30e−05 [62]
Al_2O_3-particles[b]	380.0	0.22	–	–	–	7.30e−06 [63][a]

Voce-equation : $\sigma = \sigma_0 + (\sigma_{max} - \sigma_0) * (1 - \exp(-\varepsilon/\varepsilon_0))$
E—elastic modulus (Young's modulus); ν—Poisson ratio; σ_0—yield sresss; σ_{max}—stress in saturation region of the stress–strain curve; ε_0—strain at which the change in the curvature of the stress–strain curve has been observed; α—thermal expansion coefficient.
[a] Averaged over the temperature range 20–500 °C.
[b] Elastic.

homogeneous distribution of the grey values. The tensile specimen has been mounted in a scanning electron microscope (SEM) Jeol 840 and was uniaxially loaded with a constant velocity. Digital images of chosen microstructural areas were taken before loading and after particular deformation steps. With help of an image correlation algorithm the images were compared and displacement fields as well as strain fields have been determined. A detailed description of the object grating method and in-situ tensile test in the SEM can be found in [48,49].

3.2. FE-simulation

The commercial FE-codes LARSTRAN [50] and ABAQUS [51] were used for the analysis of the elasto-plastic behaviour of the Al/Al_2O_3-composite. Six-noded triangular-shaped elements were used for the calculations. Simulations with LARSTRAN have been performed either with regular FE-meshes consisting of equal sized elements or with adaptive meshes with one-phase elements. Complex real microstructures have been mapped into the model using multiphase elements, which can be shared by two or more phases [52] as well as single (one-phase) elements, which belong only to one phase and therefore represent the location of the phase boundary and the resolution of the stress and strain gradients is better as by multiphase elements. Fig. 2 shows how experimental data have been used for creating the FE-model. 2D calculations have been controlled by experimental displacements on all four edges of the model. Mechanical data of the Al(6061) and Al_2O_3 phases are shown in Table 3.

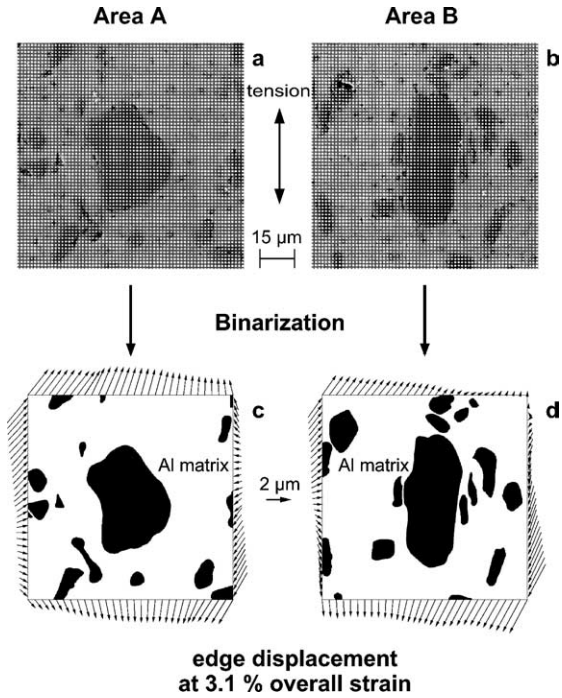

Fig. 2. SEM images (a,b) used to attain binary bitmaps (c,d) of microstructure with edge displacements (arrows).

3.2.1. Boundary conditions

Real materials, especially composites with two or more phases, show heterogeneity on different length scales. Results of FE-simulations on micro- and mesoscales are presented in this work. Modeling on the mesoscale means here simulations with models based on representative cut-outs of the microstructure. The influence of the particle distribution on the formation of shear bands and stress maps can be studied on the mesoscale.

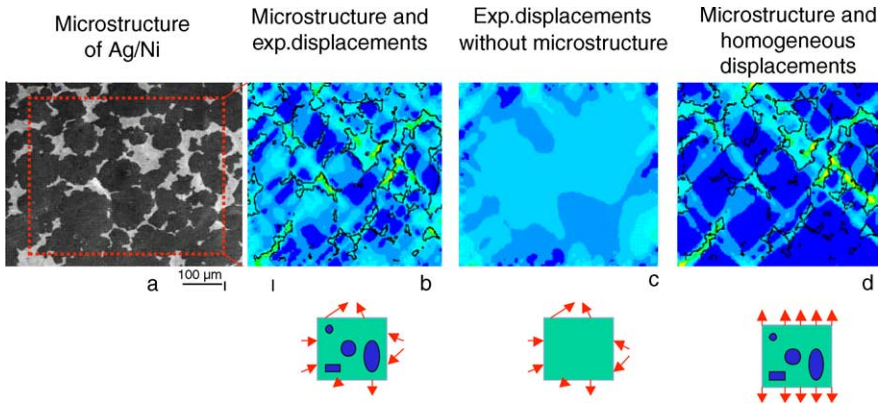

Fig. 3. Influence of the microstructure and boundary conditions on the strain maps. Calculations have been performed using Ag and Ni material data.

Models on the microscale are suitable for studying details like damage initiation, crack growth, debonding etc.

The microstructure as well as the deformation and damage processes going on in the neighbourhood of the considered microscopic cut-out do influence the deformation and the damage initiation within this area. In order to take this influence into account the experimentally determined displacements at the edges of the analysed area (Fig. 2) have been used as boundary conditions for the calculation. These displacements are assumed to carry the full information of the influence of the surroundings.

In order to show the importance of using the experimentally measured edge displacements for the simulation three distributions of effective strain were calculated in a Ag/Ni-composite (Fig. 3a) with different inputs (Fig. 3b–d). When the calculation is carried out with the measured edge displacements assuming a homogeneous material with the average properties of the composite, i.e. the two-phase composition of the material is not taken into account, the strain map is structured only near the edges of the model (Fig. 3c). This structure shows the influence of the surroundings.

This important influence gets lost if homogeneous edge displacements are applied on the real microstrucuture (Fig. 3d). The map shows the pure influence of microstructure on the distribution of strain only. The FE-simulation with real microstructure and the real values of edge displacements as boundary conditions provides the best results (Fig. 3b) [53]. In this case the calculated effective strains show most details.

3.2.2. Residual stresses

Residuals stresses in the vicinity of the reinforcement elements are generated when phases in a composite material possess different coefficients of thermal expansion (CTE) (Table 3). Al(6061)/Al_2O_3 specimens were annealed at 530 °C for 30 min, quenched to ambient temperature, annealed at 160 °C and again quenched to room temperature (Table 2). FE-calculations of the microscopic stresses under plane strain conditions for the *whole thermal cycle* (annealing at 530 °C, cooling down to ambient temperature, heating up to 160 °C and cooling down again to ambient temperature) and *only for cooling down from 160 °C* have been carried out. Because of very similar results in both simulations, only the last step of cooling down from 160 °C will be discussed here. For comparison, calculations have been made using a stress–strain curve for Al(6061) measured at ambient temperature and temperature-dependent curves. Calculated stresses ($\sigma_{xx}, \sigma_{yy}, \sigma_{zz}, \sigma_{xy}$) generated during the cooling process have been transformed from the deformed FE-mesh to an undeformed one with exactly the same shape. This is equivalent to the experimental situation: the material with residual stresses is assumed to be in an undeformed status which is used as a reference for measuring local strains after tensile deformation. Afterwards the model with and without residual

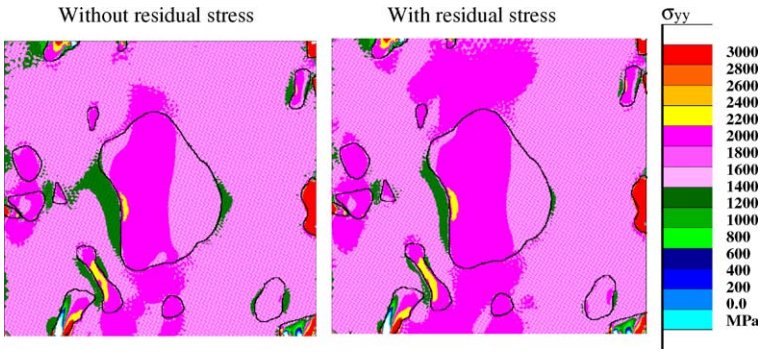

Fig. 4. Influence of the residual stresses on the stress component σ_{yy} in the loading direction after tensile deformation up to 3.1%. FE-calculation has been performed in plane strain.

stresses was mechanically strained up to 3.1%. The resulting distributions of the stress component σ_{yy} are presented in Fig. 4. The difference in the stress level is visible in the matrix on top of the centrally located particle. The experimentally observed crack along the matrix/particle surface propagating further in the matrix phase would be accelerated by residual stresses (Fig. 6).

3.2.3. Damage

A comparison between experimental and numerical results (Fig. 5) shows some differences in the distribution of the effective strains. An additional shear band appears in the experiment at the top of the big centrally located particle. Also the course of the strain concentration in the matrix at the bottom part of the particles shows differences. The analysis of the SEM figures shows the existence of voids at the top and bottom of the coarse particle (as marked in Fig. 5) as well as cracks in the Al_2O_3 inclusions. Particle cracking and microvoids around the cracked brittle particles are important damage initiation modes (Fig. 5). For modeling the damage initiation and development in particulate composite materials, it is important to know the local stress and strain distribution at the length scale of the particle size. That is in the order of a few micrometers.

3.2.3.1. Debonding at the surface matrix/particle. The debonding of the matrix/particle interface has a very important impact on the mechanical be-

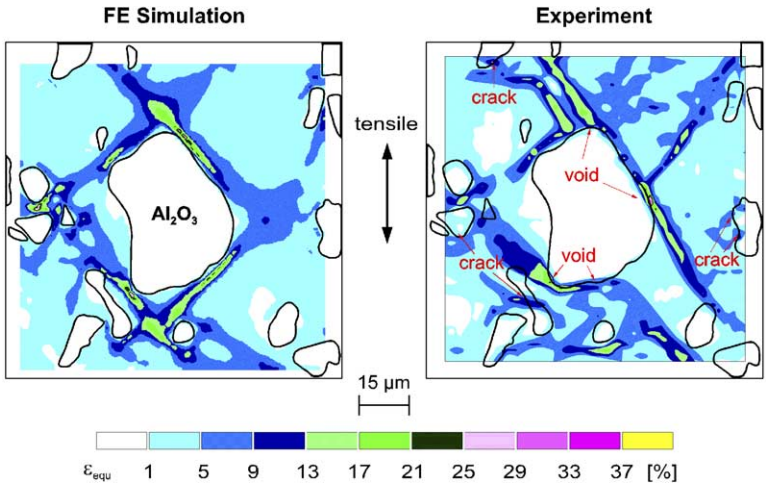

Fig. 5. Disribution of the effective strains in experiment and FE-simulation. The specimen has been strained up to 3.1% in tensile test.

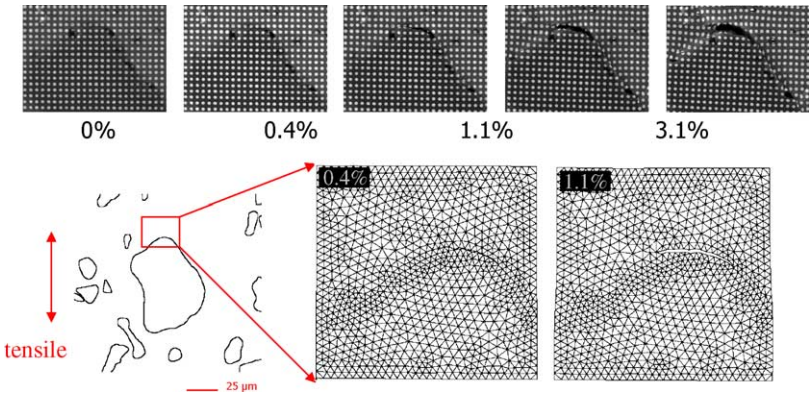

Fig. 6. Development of the crack along the matrix/particle interface during tensile loading up to an overall strain of 4.6%.

haviour of the composite material. The aim of the present part was to apply the modified criterion of Rice and Tracey [54] for modeling the interface debonding process. As an example, Fig. 6 shows the experimentally observed development of the crack along the Al/Al_2O_3 interface at five deformation steps. The crack starts from the void (at 0% deformation) and propagates at first along the interface and then in the matrix. Additionally, Fig. 6 shows FE-models with a crack on the top of the particle at 0.4% and 1.1% overall deformation. The crack propagation has been realized by double occupation of the nodes along the crack path and opening the crack by splitting nodes step by step. The crack length at subsequent steps needed for calculating the damage parameter D of Rice and Tracey has been known from the experiment. The modified damage parameter of the Rice and Tracey criterion is an integral value:

$$D = \frac{1}{A}\int_0^{\varepsilon_{pl}} e^{-B\eta}\, d\varepsilon_{pl}$$

$\eta = \sigma_H/\sigma_V$ stress triaxiality
σ_H hydrostatic stress
σ_V von Mises stress
ε_{pl} critical plastic strain
A, B material constants

As the values of A and B for Al(6061) are unknown, the corresponding material constants for pure Al: $A = 51.42$, $B = 3.48$ [55] have been used for the calculations in the present work. Using values of hydrostatic stress, von Mises stress and plastic strain, calculated by the FE-method, the damage parameter D has been calculated for all elements in the ductile matrix phase (Fig. 7). By correctly estimated A and B the damage parameter ought to reach the value of 1 when a crack starts to propagate. Fig. 7 shows the development of the damage parameter as a function of the overall strain of 0.17%; 0.29% and 0.37% for the microstructure shown in Fig. 6. The damage parameter $D = 1.477$ exceeded the critical value at an overall strain of $\varepsilon = 0.37\%$, which is very close to the experimentally observed overall strain of 0.4%. Apart from the values of A and B boundary conditions for the FE-model are playing a very important role. Fig. 8 shows a comparison between the values of local strains from the calculations with experimentally determined displacements as boundary conditions at the edges of the model (Fig. 8a) and with the displacements extracted from the bigger earlier calculated FE-model (Fig. 8b). The calculation performed with the experimental displacements gives a higher concentration of the strain in the vicinity of the crack tip as the simulation with "extracted" displacements.

4. Discussion

Failure initiates on the microscopic level. Discrete voids in the matrix or at the matrix/particle interface can grow and coalesce to the crack by an

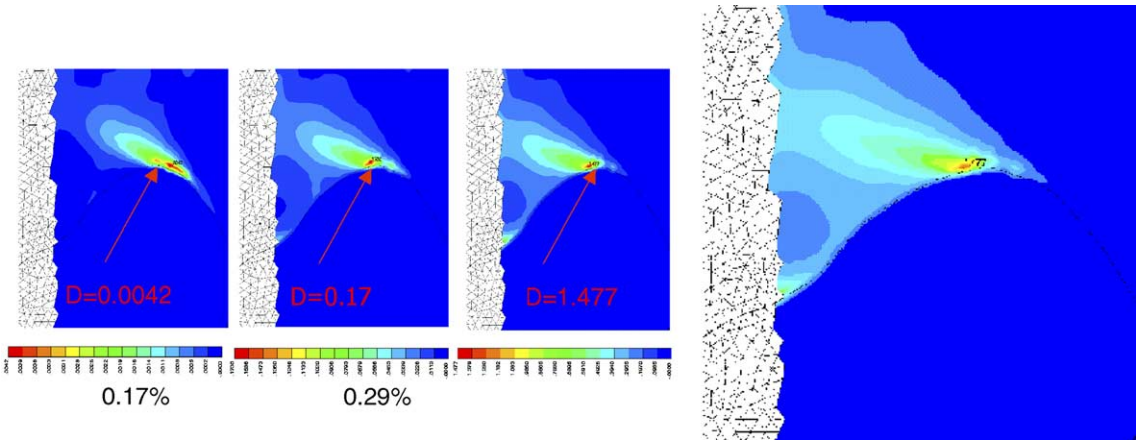

Fig. 7. Development of the damage parameter during tensile loading.

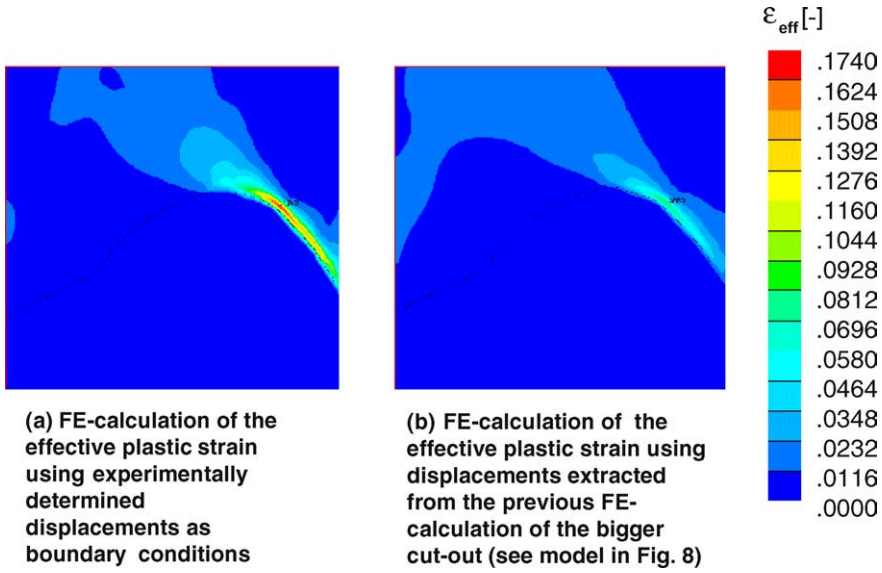

Fig. 8. Influence of the boundary conditions on plastic strain in the crack propagation model: (a) experimentally determined displacements and (b) displacements extracted from the previous FE-calculation.

unfavourable combination of external loading and internal stresses after the fabrication process. A useful prediction of the deformation and damage behaviour of an Al/Al_2O_3 component depends on how close reality and the FE-model used for the simulation are. The present work shows the way of improving the existing FE-tools in close combination with experiment by taking into consideration essential microstructural and mechanical factors.

These factors are:

- real microstructure as a basis for the simulation,
- experimental boundary conditions,

- residual stresses,
- voids or/and cracks pre-existing in the undeformed material.

The main objective of the current work is to find a damage criterion for debonding at the matrix/particle interface which appears as one of the three damage types in Al/Al_2O_3 under mechanical loading.

4.1. Microstructure

Real microstructures are mostly very complex and have a great variety of shapes, size distributions and arrangements of their components. To simplify such microstructures without losing the significant information is not easy and mostly impossible. Although simplified artificial microstructural models are very useful because of a short calculation time, they deliever mostly only tendencies of the mechanical behaviour and seldom the exact data, which could be used for instance as damage criteria. For the development of simulation tools a close connection with the experiment is required. Ideally, experimentally acquired data can be used as input for FE-calculations. Thereby are binary figures (Fig. 2) or greyscale pictures (depending on the number of phases) a sound base for FE-models.

4.2. Experimental boundary conditions

Quite contrary to the homogeneous displacements experimentally determined displacements (Fig. 2) contain the information about the surrounding when used as boundary conditions for the simulated cut-out. This enables more exact calculation of the stress and strain patterns in the matrix phase (see Fig. 3).

4.3. Residual stresses

Tensile residual stresses in the matrix phase before the application of the external loading could be seen as a kind of defects [56] which may initiate a microcrack when a composite is mechanically loaded. Thereby the geometrical shape of the reinforcement is of importance. This is an additional argument for modeling of real structures instead of simplified ones.

Reetz [57] has measured by neutron diffraction the residual stresses in Al_2O_3 particles in Al(6061) with 10%, 15% and 22% of the ceramic phase in the undeformed state and after compression. He detected the stress of −200 MPa in the hard phase (15% Al_2O_3) before the deformation and a decreasing stress from −200 to −50 MPa after 25% compression. The FE-calculations of the residual stresses in the Al_2O_3 particle (model presented in Fig. 4) performed in the present work in undeformed specimen delivered the values between −30 and −167 MPa. The maximum of the effective plastic strain in the matrix near the interface has been found to be 0.5%. It points on the plastic flow in the matrix as a result of the cooling down process. Additional tensile loading increased the σ_{yy} stress component (in the loading direction) up to maximal 2000 MPa in the ceramic particle at the macroscopic strain of 3.1%. At this deformation degree no significant difference in the stress level in the inclusion "with" and "without residual stress" has been observed. The average value of the breakage stress for Al_2O_3 is about 1500 MPa. At the intact interface one can expect an unbroken load transfer to the particle causing high stress concentration inside and finally inclusion damage. In the experiment two interface cracks at the bottom and top poles of the inclusion have been observed. They interrupted the load transfer, changed the stress partitioning between the reinforcement and the matrix and prevent the Al_2O_3 particle from damage. In the FE-model used for the calculation of the residual stresses there was no debonding at this time.

4.4. Debonding

The additional shear band at the top of the Al_2O_3 (Fig. 5) is the result of the interface crack. The FE-study on how cracks in the microstructure change the strain and stress pattern [64] confirms this result. In the FE-analysis presented in Fig. 5 the intact microstructure has been modeled. The Rice and Tracey criterion for damage is valid for a ductile, plastic deformable phase. The usage of this criterion for the interface crack was an attempt to

extend the usability for debonding, that means for the contact surface between the elastic and elasto-plastic materials. The crack starts from a void (Fig. 6) and its propagation is connected with a high strain concentration at the crack tip (Fig. 8a). The crack growth is facilitated by the shear band in the matrix along the right side of the particle (Fig. 5). Damage parameter very close to 1 reached in the presented FE-calculations encourages the authors of this paper to the statement, that the interface crack can be described by the criterion of Rice and Tracey. The experimentally observed crack (Fig. 6) runs along the interface in the first stage of the deformation, leaves the interface and propagates further in the matrix. This fact point out that the interface strength is probably slightly below that of the matrix strength. In the case of a significantly stronger interface no debonding should occur. For a significantly weaker interface the crack should not change its path into the matrix at the beginning of the deformation.

The strength of the ceramic/metallic matrix interface is an important factor by designing ceramic reinforced metal matrix composites with a high crack resistance. Very strong interfaces (high value of the shear strength along the interface) cause high concentrations of stresses in the particles (or fibres) and, therefore, a premature failure of the component. Weak interfaces change the crack path and cause debonding along a certain length of the particles (or fibres). This process prevents too high increase of stress in the particles, but on the other hand too weak interfaces break the stress transfer into the ceramic phase. The derivation of a criterion for particle cracking seems to be more difficult. Existing, statistically distributed defects in the ceramic phase initiate cracks. The probability to find such a defect depends on the volume of the ceramic particles. Coarse, elongated, favourable to the loading direction oriented particles break earlier than small, roundish shaped ones.

A competition between the crack growth in the particles and along the interface seems to exist. The compromise between these both processes could probably lead to materials with an improved profile of properties.

5. Conclusions

The following conclusions can be drawn from the results of the present paper:

1. The improvement of FE-models for the prediction of the mechanical behaviour of MMCs has been performed by incorporating the following factors
   - real microstructure models,
   - experimental boundary conditions,
   - thermal residual stresses,
   - voids and cracks in the undeformed state,
   - damage criterion for the correct prediction of the crack development.
2. Residual stresses cause tensile stresses in the matrix phase near the Al/Al_2O_3 interface and can accelerate interface debonding.
3. Interface cracks interrupt the load transfer to the reinforcement phase and change the stress partitioning between the phases of the composite.
4. Interface cracks change the strain pattern in the matrix phase, new shear bands initiate near the interface crack.
5. The damage criterion of Rice and Tracey can be used for the prediction of the development and the location of the interface crack.
6. Based on the interface crack path analysis, conclusion about the comparable values of interface and matrix strength in Al/Al_2O_3 used in the presented work, can be drawn.

Acknowledgements

This work was performed in frame of the Research Group "Investigation of the deformation behaviour of heterogeneous materials by direct combination of experiment and computation", subproject DFG Schm 746/16-1, 2, 3 and DFG Fi 686/1-1, 2, 3. The authors gratefully acknowledge the financial support by the Deutsche Forschungsgemeinschaft (DFG).

The authors would like to express special thanks to Mr. Roland Mellert for his help with the FE-mesh preparation procedure.

References

[1] G. Bao, A micromechanics model for damage in metal matrix composites, in: Damage Mechanics and Localization, AMD-Vol.142/MD-Vol. 34, ASME, 1992.

[2] G. Bao, Damage due to fracture of brittle reinforcements in a ductile matrix, Acta Metall. Mater. 40 (10) (1992) 2547–2555.

[3] J. Llorca, C. González, Microstructural factors controlling the strength and ductility of particle reinforced metal–matrix composites, J. Mech. Phys. Solids 46 (1) (1998) 1–28.

[4] J.R. Brockenbrough, F.W. Zok, On the role of particle cracking in flow and fracture of metal matrix composites, Acta Metall. Mater 43 (1) (1995) 11–20.

[5] M.-O. Nandy, S. Schmauder, B.-N. Kim, M. Watanabe, T. Kishi, Simulation of crack propagation in Al_2O_3 particle–dispersed SiC Composites, J. Eur. Cer. Soc 19 (1998) 329–334.

[6] J. Yang, C. Candy, M.S. Hu, F. Zok, R. Mehrabian, A.G. Evans, Effects of damage on the flow strength and ductility of a ductile Al alloy reinforced with SiC particulates, Acta Metall. Mater. 38 (1990) 2613–2619.

[7] M. Seidenfuß, Untersuchungen zur Beschreibung des Versagensverhaltens mit Hilfe von Schädigungsmodellen am Beispiel des Werkstoffes 20 MnMoNi 5 5, Dissertation, Staatliche Materialprüfungsanstalt (MPA) Universität Stuttgart, 1992.

[8] N. Lippmann, A. Lehman, Th. Steinkopff, H.-J. Spies, Modelling of the fracture behaviour of high speed steels under static loading, Comput. Mater. Sci. 7 (1996) 123–130.

[9] A.F. Plankensteiner, H.J. Böhm, F.G. Rammerstorfer, V.A. Buryachenko, Hierarchical modelling of the mechanical behaviour of high speed steels as layer-structured particulate MMCs, J. de Phys. III (1996) 395–402.

[10] H.J. Böhm, W. Han, Comparisons between three-dimensional and two-dimensional multi-particle unit cell models for particle reinforced MMCs, Model. Simul. Mater. Sci. Eng. 9 (2) (2001) 47–65.

[11] M. Geni, M. Kikuchi, Damage analysis of aluminium matrix composite considering nonuniform distribution of SiC particles, Acta Metall. Mater. 46 (1998) 3125–3133.

[12] A.B. Ljungberg, C. Chatfield, M. Hehenberger, B. Sundström, Estimation of the plastic zone associated with cracks in cemented carbides, in: Proc. 2nd Int. Conf. Sci. of Hard Mater. (Rhodes/Greece) Inst. Phys. Conf. Ser., vol. 75, 1986, p. 619.

[13] V. Tvergaard, Report des Department of Solid Mechanics, The Technical University of Denmark, Lyngby, Denmark, 1990.

[14] P. Lipetzky, S. Schmauder, Crack–particle interaction in two-phase composites, Part I: particle shape effects, Int. J. Fract. 65 (1994) 345–358.

[15] P. Lipetzky, S. Schmauder, Particle geometry effects on a stationary crack, in: T. Chandra, A.K. Dhingra (Eds.), TMS-AIME, Advanced Composites '93, Int. Conf. Adv. Comp. Mats., The Minerals, Metals and Materials Society, 1993, pp. 289–294.

[16] P. Lipetzky, S. Schmauder, H. Fischmeister, Geometrical factors related to composite microcracking, Comput. Mater. Sci. 1 (1993) 325–332.

[17] W.H. Müller, S. Schmauder, Stress-intensity factors of r-cracks in fiber-reinforced composites under thermal and mechanical loading, Int. J. Fract. 59 (1993) 307–343.

[18] M. Dong, S. Schmauder, Modelling of metal matrix composites by a self-consistent embedded cell model, Acta Metall. Mater. 44 (1996) 2465–2478.

[19] U. Weber, Arbeitsbericht zum Projekt, Mikrostrukturelle Modellierung zum Einfluß der Eigenspannungsentwicklung auf die Schädigung bei der Kaltmassivumformung mehrphasiger Werkstoffe im DFG SSP, Erweiterung der Formgebungsgrenzen bei Umformprozessen, MPA Universität Stuttgart, 1999.

[20] E. Soppa, S. Schmauder, G. Fischer, Numerical and experimental investigations of the influence of particle alignment on shear band formation in Al/SiC, in: 19th Risoe Int. Symp. on Material Science, Risø National Laboratory, Roskilde, DK, 7–11 September 1998, pp. 499–504.

[21] L.L. Mishnaevsky Jr., N. Lippmann, S. Schmauder, P. Gumbsch, In-situ observation of damage evolution and fracture in AlSi7Mg0.3 cast alloys, Eng. Fract. Mech. 63 (1999) 395–411.

[22] H. Dietzhausen, M. Dong, S. Schmauder, Numerical simulation of acoustic emission in fiber reinforced polymers, Comput. Mater. Sci. 13 (1998) 23–30.

[23] S. Hönle, M. Dong, L. Mishnaevsky Jr, S. Schmauder, FE-simulation of damage evolution and crack growth in two phase materials, in: A. Bertram et al. (Eds.), Proc. 2nd Europ. Mechanics of Materials Conf. (Euromech-Mecamat), Magdeburg, 1998, pp. 189–196.

[24] S. Hönle, Micromechanical Modelling of Deformation and Fracture of Graded WC/Co Hard Metals, Dissertation, Universität Stuttgart, 1998.

[25] S. Hönle, S. Schmauder, Micromechanical simulation of crack growth in WC/Co using embedded unit cells, Comput. Mater. Sci. 13 (1998) 56–60.

[26] J. Wulf, in: Neue Finite-Elemente-Methoden zur Simulation des Duktilbruchs in Al/SiC, Reihe 18, Nr. 173, VDI Verlag, Düsseldorf, 1995.

[27] O. Mintchev, J. Rohde, S. Schmauder, Mesomechanical simulation of crack propagation through graded ductile zones in hardmetals, Comput. Mater. Sci. 13 (1998) 81–89.

[28] E. Soppa, S. Schmauder, Numerical investigations of the influence of particle alignment on shear band formation in Al/SiC, in: A. Streckhardt (Ed.), Proc. XXV. Int. FEM-Congress, Baden-Baden, 16–17 November 1998, Kongreßorganisation, Ennigerloh, 1998, pp. 149–160.

[29] G. Fischer, E. Soppa, S. Schmauder, Y.-L. Liu, Localization of strain in real microstructural areas of the particle reinforced metal–matrix composite Al 6061-10% Al_2O_3, in: 19th Risø Int. Symp. on Material Science, Risoe National

Laboratory, Roskilde, DK, 7–11 September 1998, pp. 261–266.
[30] E. Soppa, in: Experimentelle Untersuchung des Verformungsverhaltens zweiphasiger Werkstoffe, Reihe 5, Nr. 408, VDI Verlag, Düsseldorf, 1995.
[31] P. Leßle, M. Dong, E. Soppa, S. Schmauder, Simulation of interpenetrating microstructures by self consistent matricity models, in: T. Winkler, A. Schubert (Eds.), Materials Mechanics, Fracture Mechanics, Micro Mechanics. An Anniversary Volume in Honour of B. Michels 50th Birthday, Fraunhofer IZM Berlin, Chemnitzer Werkstoffmechanik GmbH, Chemitz, 1999, pp. 456–461.
[32] J. Rohde, Mesoskopische Modellierung des Versagensverhaltens beschichteter gradierter Hartmetalle, Dissertation an der Universität Stuttgart, 1998.
[33] J. Rohde, S. Schmauder, G. Bao, Mesoscopic modelling of gradient zones in hardmetals, Comput. Mater. Sci. 7 (1996) 63–67.
[34] P. Doumalin, Microextensométrie Locale par Corrélation d'Image Numériques, PhD Thesis, École Polytechnique, Paris, 2000.
[35] A.M. Gokhale, S. Yang, Application of image processing for simulation of mechanical response of multi-length scale microstructure of engineering alloys, Metall. Mater. Trans. 30A (1999) 2369–2381.
[36] A.M. Gokhale, Estiamtion of bivariate size and orientation distribution of microcracks, Acta Mater. 44 (2) (1996) 475–485.
[37] S. Yang, A. Tewari, A.M. Gokhale, Modelling of non-uniform spatial arrangement of fibers in a ceramic matrix composite, Acta Mater. 45 (7) (1997) 3059–3069.
[38] H. Agrawal, A.M. Gokhale, S. Graham, M.F. Horstemeyer, D.J. Bamman, Rotations of brittle particles during plastic deformation of ductile alloys, Mater. Sci. Eng. A 328 (2002) 310–316.
[39] M.D. Dighe, A.M. Gokhale, M.F. Horstemeyer, Effect of loading condition and stress state on damage evolution of silicon particles in an Al–Si–Mg base cast alloy, Metall. Mater. Trans. A 33A (2002) 555–565.
[40] M.F. Horstemeyer, A.M. Gokhale, A void-crack nucleation model for ductile metals, Int. J. Solids Struct. 36 (1999) 5029–5055.
[41] E. Le Pen, D. Baptiste, Prediction of the fatigue-damaged behaviour of Al/Al_2O_3 composites by a micro–macro approach, Compos. Sci. Technol. 61 (2001) 2317–2326.
[42] G.K. Hu, G. Guo, D. Baptiste, A micromechanical model of influence of particle fracture and particle cluster on mechanical properties of metal matrix composites, Comput. Mater. Sci. 9 (1998) 420–430.
[43] J. Fitoussi, G. Guo, D. Baptiste, A statistical micromechanical model of anisotropic damage for S.M.C. composites, Compos. Sci. Technol. 58 (1998) 759–763.
[44] K. Derrien, J. Fitoussi, G. Guo, D. Baptiste, Prediction of the effective damage properties and failure properties of non linear anisotropic discontinuous reinforced composites, in: C.A. Mota Soares et al. (Eds.), Mechanics of Composite Materials and Structures, 1999, pp. 131–150.
[45] K. Derrien, D. Baptiste, D. Guedra-Degeorges, J. Foulquier, Multiscale modeling of the damaged plastic behaviour and failure of Al/SiCp composites, Int. J. Plast. 15 (1999) 667–685.
[46] J. Fitoussi, G. Guo, D. Baptiste, Determination of a tridimensional failure criterion at the fibre/matrix interface of an organic-matrix/discontinuous-reinforcement composite, Comops. Sci. Technol. 56 (1996) 755–760.
[47] Information of ARC Leichtmetall Kompetenzzentrum Ranshofen GmbH.
[48] Y.L. Liu, G. Fischer, Local strain fields in particulate metal matrix composites characterized by the object grating technique, in: M.L. Scott (Ed.), Proc. ICCM-11, vol. 3, Australian Composite Structures Society, pp. 1–9.
[49] H.-A. Crostack, G. Fischer, E. Soppa, S. Schmauder, Y.-L. Liu, Localization of strain in metal matrix composites studied by a scanning electron microscope-based grating method, J. Microsc. 201 (2001) 171–178.
[50] LARSTRAN User's Manual, Part V Element Library, LASSO Ingenieurgesellschaft R. Dietz, U. Hindenlang, A. Kurz, Markomannenstraße 11, D-70771 Leinfelden-Echterdingen, November 1993.
[51] Hibbit, Karlson and Sorensen Inc., ABAQUS 6.2-1, Pawtucket, RI, USA, ABACOM Software GmbH, Aachen.
[52] Th. Steinkopff, M. Sautter, Simulation of the elasto-plastic behaviour of multiphase materials by advanced finite element techniques, Comput. Mater. Sci. 4 (1995) 10–22.
[53] P. Doumalin, M. Bornert, E. Soppa, Computational and experimental investigations of the local strain field in elastoplastic two-phase materials, in: D. Miannay, P. Costa, D. Francois, A. Pineau (Eds.), Advances in Mechanical Behaviour, Plasticity and Damage, EUROMAT 2000, vol. 1, pp. 323–328.
[54] J. Rice, D.M. Tracey, On the ductile enlargement of voids in triaxial stress fields, J. Mech. Solids 17 (1969) 201–217.
[55] Private information from Dr. Seidenfuss and Dr. Zhu, MPA Universität Stuttgart, Germany.
[56] S. Ho, A. Saigal, Thermal residual stresses and mechanical behaviour of cast SiC/Al composites, Mater. Sci. Eng. A 183 (1994) 39–47.
[57] B. Reetz, Untersuchungen zur Verformung von partikelverstärkten Metallmatrix-Teilchenverbundwerkstoffen am Beispiel von $AA6061 + Al_2O_3$, Diplomarbeit, Hahn–Meitner-Institut, Berlin, 2001, 60 p.
[58] H. Li, J.B. Li, L.Z. Sun, S.X. Li, Z.G. Wang, Effect of low temperature treatment regime on residual stress state near interface in bonded SiC/6061 Al compounds, Mater. Sci. Eng. A 221 (1996) 179–186.
[59] Private information from Y.-L. Liu, Risø National Laboratory; PO Box 49, DK-4000 Roskilde, Denmark.
[60] M. Jain, S.R. MacEwen, L. Wu, Finite element modelling of residual stresses and strength differential effect in discontinuously reinforced metal matrix composites, Mater. Sci. Eng. A 183 (1994) 111–120.
[61] J.-Y. Buffière, E. Maire, P. Cloetens, G. Lormand, R. Fougères, Characterization of internal damage in a MMCp

using X-ray synchrotron phase contrast microtomography, Acta Mater. 47 (5) (1999) 1613–1625.
[62] Leichtmetallkompetenzzentrum Ranshofen GMBH "Werkstoffblätter".
[63] D. Munz, T. Fett, Mechanisches Verhalten keramischer Werkstoffe, Springer-Verlag, 1989.
[64] E. Soppa, U. Weber, S. Schmauder, G. Fischer, Spannungs- und Dehnungskonzentrationen in Al/Al_2O_3—Verbundwerkstoffen verursacht durch Schädigungsprozesse, in: H.P. Degischer (Ed.), 14. Symposium "Verbundwerkstoffe und Werkstoffverbunde", Wien, 2003, pp. 581–586.